Title

MR-based techniques for intracortical vessel visualization and characterization: understanding the impact of microvascular disease on skeletal health

Journal

Current Opinion in Endocrinology Diabetes and Obesity, 30(4)

ISSN

1752-296X

Authors

Löffler, Maximilian T
Wu, Po-Hung
Kazakia, Galateia J

Publication Date

2023-08-01

DOI

10.1097/med.0000000000000819

Peer reviewed

HHS Public Access

Author manuscript

Curr Opin Endocrinol Diabetes Obes. Author manuscript; available in PMC 2024 August 01.

Published in final edited form as:

Curr Opin Endocrinol Diabetes Obes. 2023 August 01; 30(4): 192–199. doi:10.1097/MED.0000000000000819.

MR-based techniques for intracortical vessel visualization and characterization: understanding the impact of microvascular disease on skeletal health

Maximilian T. Löffler[1,2,3], **Po-Hung Wu**[1], **Galateia J. Kazakia**[1]

[1]Department of Radiology and Biomedical Imaging, University of California, San Francisco, CA, USA; 185 Berry St, Suite 350, San Francisco, CA 94107, Tel: (415) 514-9655

[2]Department of Diagnostic and Interventional Radiology, University Medical Center Freiburg, Freiburg im Breisgau, Germany

[3]Department of Diagnostic and Interventional Neuroradiology, School of Medicine, Klinikum rechts der Isar, Technical University of Munich, Munich, Germany

Abstract

Purpose of review: The relationships between bone vasculature and bone microstructure and strength remain incompletely understood. Addressing this gap will require in vivo imaging capabilities. We describe the relevant vascular anatomy of compact bone, review current magnetic resonance imaging (MRI)-based techniques that allow in vivo assessment of intracortical vasculature, and finally present preliminary studies that apply these techniques to investigate changes in intracortical vessels in aging and disease.

Recent findings: Ultra-short echo time MRI (UTE MRI), dynamic contrast enhanced MRI (DCE-MRI), and susceptibility-weighted MRI techniques are able to probe intracortical vasculature. Applied to patients with type 2 diabetes, DCE-MRI was able to find significantly larger intracortical vessels compared to non-diabetic controls. Using the same technique, a significantly larger number of smaller vessels was observed in patients with microvascular disease compared to those without. Preliminary data on perfusion MRI showed decreased cortical perfusion with age.

Summary: Development of in vivo techniques for intracortical vessel visualization and characterization will enable the exploration of interactions between the vascular and skeletal systems, and further our understanding of drivers of cortical pore expansion. As we investigate potential pathways of cortical pore expansion, appropriate treatment and prevention strategies will be clarified.

Keywords

MRI; cortical; porosity; vessel; vasculature; in vivo clinical imaging; perfusion

Correspondence: Maximilian T. Löffler, m_loeffler@web.de.

Conflicts of interest

The authors declare no conflict of interest.

Introduction

Cortical bone microstructure is a critical aspect of skeletal health. Cortical bone constitutes approximately 80% of skeletal tissue mass and carries the majority of the load in the appendicular skeleton. Cortical bone strength, stiffness, and fracture toughness – and therefore propensity to fracture – are determined to a large extent by the amount of porosity present in the cortex [1,2,3]. Increased porosity is strongly associated with age-related skeletal fragility [4]. Increased porosity is also a hallmark structural feature of diabetic bone disease and chronic kidney disease, which manifest in substantially higher fracture risk compared to healthy controls.

The two main components of cortical pore space are adipocytes and vessels, both of which are known to impact bone turnover [5,6]. Both of their main constituents, fat and water, are ideal contrast materials for magnetic resonance imaging (MRI) because of their high hydrogen content. The historical understanding of cortical pore content was focused on vessels within osteonal pore space and marrow adipocytes within transition zone ‘trabecularized’ endocortical spaces. However, our recent histological and imaging studies [7,8] have documented that vessels and adipocytes have a more diverse distribution throughout the intracortical pore space than previously appreciated. In histological samples from cadaver specimens (including donors with cardiovascular disease and type 2 diabetes), we found evidence of large, sub-periosteal pores containing primarily adipocytes, with sparse evidence of capillaries and connective fibrous tissue (Fig. 1). In contrast, typical osteonal pore space contained primarily vascular and neuronal structures with surrounding connective fibrous tissue anchoring vessels to canal walls. Therefore, the common assumption that intracortical porosity is equivalent to vascular space, and that probing water content (as in ultrashort echo-time [UTE] MRI) provides an adequate measure of porosity, may be invalid in patients with skeletal involvement of vascular or metabolic disease.

Visualization and identification of the biological systems interacting with cortical porosity will expand our understanding of the mechanisms driving pathological porosity. Adipocytes interact with bone morphology through both passive and active mechanisms. Bone marrow mesenchymal stem cells are the common progenitors of both adipocytes and osteoblasts; increase in adipocyte differentiation, therefore, comes at the expense of osteoblast differentiation [9]. Furthermore, bone remodeling is actively modulated by adiponectin synthesized by bone marrow adipocytes [10]. Vessels interact with bone morphology through the coupling of angiogenesis and osteogenesis [11,12]. Specialized capillaries in the murine skeletal system built of endothelial cells named type H for their high expression of CD31 and Endomucin mediate bone growth through molecular signaling, communication with osteoprogenitor cells, and their ability to create microenvironments for adult stem cell populations [13]. These interactions on a molecular and cellular level are expected to translate to alterations of bone microstructure via the bone-vascular axis [12]. Therefore, microvascular disease may effect cortical microstructural changes in aging and pathologic conditions. Visualization of intracortical vasculature and longitudinal changes preceding or accompanying local bone changes will let us better understand how vasculature interacts with bone on a microstructural level.

As we investigate these potential pathways of cortical pore expansion, appropriate treatment and prevention strategies will be clarified. Identifying mechanisms of pore growth will point towards treatment or prevention of high porosity, for example interventions focused on directing mesenchymal stem cell differentiation towards osteoblastogenesis or targeting the adiponectin pathway. Alternatively, increased porosity due to vascular drivers might indicate modulation of vasoregulators or anti-angiogenic therapy as used to combat neovascularization and bone erosion in rheumatoid arthritis.

Current research highlights how angiogenesis and osteogenesis go hand in hand on a cellular and molecular level, but these processes remain incompletely understood [12]. Even less is known about how alterations in bone vasculature can affect bone microstructure and strength. In this context, we review current literature on MR-based techniques that allow in vivo assessment of intracortical vasculature. First, we describe the vascular anatomy of human long bones with focus on compact bone. Then, we describe MRI techniques to visualize intracortical vessels or evaluate vascularization. Finally, we present preliminary studies that apply these techniques to investigate changes in intracortical vessels in aging and disease.

Anatomy of bone vasculature

It is critical to review current understanding of bone vasculature in order to validate in vivo imaging that is operating at its resolution limit. What do we know about blood supply of long bones and intracortical vessels? Blood supply to bone is essential to maintain its ability to grow, remodel, and heal. Through blood vessels oxygen, nutrients, and cells are distributed, and waste products are removed. The vasculature is continuously reconfigured in cortical bone depending on the demands of bone remodeling [14].

The understanding of osseous blood supply saw major advances in the 20th century led by Brooks, Trueta, and their colleagues [15]. However, studying real-time physiology in compact bone is technically very difficult due to its inaccessibility. Blood flow in long bones is primarily centrifugal, at least in young adults [15]. Arterial blood is brought to the bone via a central diaphyseal nutrient artery, a few metaphyseal, and epiphyseal nutrient arteries that pass from the outer cortex to the medullar cavity. There, they branch into arterioles to both supply the medullary bone and penetrate back into the cortical bone. This centrifugal supply from the endosteal side constitutes the larger portion of intracortical blood supply in human adults. A smaller portion of arterial blood is supplied by penetrating arterioles from the periosteal side. Arterial vessels from inside and outside (endosteal and periosteal) can anastomose in the cortical bone before they drain via small venous vessels into the central venous sinus in the medullary cavity and ultimately through emissary veins to the outside. At the smallest scale, intracortical capillaries are central to functional bone units (osteons). Osteons are cylindrically shaped structures arranged along the long axis of bone and parallel to the surface. Single or paired capillaries in the osteonal central canals (Haversian canals) connect to other canals via obtuse bifurcating canals (Volkmann’s canals). In summary, arterial blood supply to intracortical capillaries is provided from the endosteal and periosteal surfaces, whereas venous drainage passes through the central venous sinus.

This concept of bone vascularity in human long bones was recently challenged by describing a network of trans-cortical vessels (TCV) in mice [16] that contributes 80% of arterial and 59% of venous blood flow. A similar network of TCVs was also described in the murine skull [17]. Of note, compact bone in mice mainly consists of woven bone with poorly organized osteocytes in contrast compact bone in humans with concentrical alignment of osteocytes in osteons [18]. The higher organizational level of human compact bone (=osteons) is likely paralleled in the vascular system with a larger number of branch points in the vascular tree. Therefore, we can expect different contributions of capillaries, arterioles, and nutrient arteries to total blood flow in humans compared to mice. This is relevant insofar as smaller nutrient arteries can be visualized in clinical MRI (Table 1).

Imaging techniques for identification and visualization of intracortical vessel

First, X-ray based and ultrasound related imaging techniques are presented, then, several MRI techniques that can visualize vessels or assess vascularization in cortical bone are reviewed. Techniques with and without intravenous administration of specific contrast materials are included.

Non-MRI imaging

Computed tomography (CT) angiography and perfusion imaging have long been available. Intravascular injection of iodinated contrast agent is required to visualize vasculature or well-perfused tissue by increasing attenuation. Mineralized bone and iodine contrast material share high attenuation coefficients that make it difficult to distinguish vasculature from compact bone. In addition, diameters of typical intracortical vessels are below the resolution of clinical multidetector CT scanners. Micro CT (μCT) provides higher nominal resolution as high as 700 nm to visualize small intracortical vessels [21,22]. Phase-contrast synchrotron-based CT can achieve even higher nominal resolution of 325 nm and increased image contrast due to sample-induced phase shift that allows individual capillaries to imaged [23]. However, access to both high resolution CT techniques is limited and they allow only ex-vivo or animal scans. In clinical practice, exposure to ionizing radiation and adverse effects to iodine contrast limit utilization of CT. Several research groups used sonography to assess cortical perfusion and vasculature by injecting ultrasound contrast agent or applying refraction-corrected techniques that enhance blood vessels [24,25]. However, sonography suffers from a lack of 3D anatomical information and limited imaging depth.

Ultrashort echo-time MRI

MRI can provide 3D anatomical information with high spatial resolution without using ionizing radiation. Protons from water molecules are excited by a radiofrequency pulse in a strong magnetic field. Cortical bone contains water protons in the form of bound water (bound to hydroxyapatite and collagen in the extracellular matrix) and pore water (unbound in the cortical pore space, particularly within vessels). Both forms of water protons have very short transverse relaxation times (T2*) of less than 0.05 ms that require ultrashort echo-time (UTE) sequences for imaging [26]. Total bone water can be calculated by comparing the UTE signal in cortical bone to a reference phantom. By fitting a two-component model

of total bone water, pore water can be extracted as an indirect (and incomplete) measure of cortical porosity [26,27,28]. More efficient approaches to evaluate cortical porosity using UTE sequences have been developed. Two different MRI sequences – UTE to detect total bone water and standard echo time (TE= 2.2 ms) to detect pore water – are acquired to calculate a porosity index (PI) from their signal ratio [29]. In a different approach, an inversion recovery UTE (IR-UTE) sequence that suppresses the signal from pore water is combined with a UTE sequence to calculate a suppression index (SI), an inverse indicator of cortical porosity [30]. A caveat of these approaches is that a significant portion of intracortical porosity can contain fat rather than vasculature (as detailed in the introduction [7,8]) and therefore these metrics of pore water cannot fully represent intracortical porosity.

Dynamic Contrast-enhanced MRI

Dynamic contrast-enhanced MRI (DCE-MRI) uses gadolinium-based or superparamagnetic iron oxide-based contrast agents to evaluate vessels and tissue perfusion [31]. These contrast agents exhibit strong paramagnetism, which shortens the spin-lattice relaxation time (T1), thus, increasing MR signal intensity. DCE-MRI acquires a time series of MRI data that measures temporal change of the MRI signal after intravenous contrast injection. Vessel and tissue perfusion can be analyzed by extracting features from the enhancement curve or fitting of pharmacokinetic models to it. Feasibility to assess cortical bone perfusion using 2D UTE or IR-UTE sequences was demonstrated [32]. IR-UTE can be favored for perfusion imaging in cortical bone because of higher signal enhancement compared to UTE sequences.

Although cortical bone has minimal signal in conventional MRI sequence, its perfusion and larger-scale vasculature can be assessed when the analysis is confined to the cortical pore space (Fig. 2). Therefore, a multimodal imaging protocol was developed using a cortical pore mask derived from high-resolution peripheral quantitative CT (HR-pQCT) to analyze vessels and perfusion in the cortical pore space using DCE-MRI [33]. The MRI protocol utilized a spoiled gradient echo sequences (SPGR) with circular cartesian undersampling reconstruction (CIRCUS) to increase temporal resolution to 30 s. This imaging technique was able to resolve vessels with a diameter larger than 200 μm in a virtual phantom study. Time-of-flight (TOF) MR angiography using a ultra-high field (7T) MRI scanner has also been used to visualize small cortical capillaries in a single human subject [16]. However, access to 7T scanners is very limited and side-effects of high magnetic field strengths hinder its clinical use.

Susceptibility-weighted MRI

While contrast-enhanced MRI has many advantages for detecting and visualizing cortical bone vasculature, it cannot be applied in all cases. For example, gadolinium-based contrast agent may damage the health of patients with poor renal function. Currently, there is no established contrast-free MRI imaging protocol to visualize cortical bone vasculature. However, there are a number of phase change MRI sequences that have potential for visualizing bone vasculature without contrast enhancement. Susceptibility weighted imaging (SWI) is widely used in neuroimaging for displaying brain vessels and iron deposition [34]. SWI has also been utilized in cartilage canal vessel imaging [35,36]. Compounds such as iron distort the local magnetic field and then change phase. This creates a tissue-inherent

contrast that can be exploited to create a phase mask indicating the susceptibilities of tissue. Nissi et al. first developed a SWI protocol on a ultra-high-field MRI scanner for visualizing cartilage canal vessels in porcine epiphyseal growth cartilage [37]. In this study, they tested their protocols on specimens and on in vivo porcine subjects with 9.4T, 7T, and 3T MRI scanners. The image resolution of 9.4T can reach 100 μm, while the image resolution of 7T and 3T can reach ~250 μm and 375 μm with the manufacturer's settings and processing software. By comparison to gold standard μCT images, their results demonstrated the ability to visualize cartilage canals using SWI. After developing the SWI protocol, Nissi et al. further improved their protocol by using quantitative susceptibility mapping (QSM), which utilizes multiples echoes to calculate local susceptibility and generate weighted signal enhancement [38], improving the sensitivity of susceptibility change detection [39,40]. Based on their results, QSM improves spatial resolution of canal visualization. However, this technique faces challenges in cortical bone, which causes magnetic field inhomogeneity under standard TE. Further optimization of MRI sequences is required to make SWI and QSM feasible in visualizing cortical vasculature.

Application of imaging techniques for intracortical vessels

Studying intracortical vessels with clinical MRI can help to identify new biomarkers associated with skeletal health. These markers of bone vascularity could be used in preclinical human and animal studies and, potentially, in clinical trials to investigate treatment interventions targeting bone disease. As described, MRI of intracortical vessels faces technical and safety limitations that pertain to image resolution, scan time, and adverse contrast media effects. Due to these challenges, in vivo MRI studies of intracortical vessels are sparse.

Human studies of intracortical vessels

Visualization of intracortical vessels with sizes as small as 53 μm diameter in the human femoral neck was demonstrated using ultra-high-field (7T) time-of-flight MR angiography [16]. However, ultra-high-field MRI is not likely to be deployed in broad clinical application due to physiologic side effects, long scan times, and other technical challenges [41]. Despite resolution limitations [42] intracortical vessels can be partly visualized in vivo in humans using clinical 3T MRI. A first feasibility study utilized DCE-MRI on a clinical 3T scanner to image intracortical vessels in the distal tibia of 19 volunteers (10 men, 9 women, mean age 63 ± 5 years) with low bone mass (T-scores -2.5 to -1.0) [33]. Using a vessel detection algorithm this study found a mean vessel volume of 0.032 mm^3 and a mean vessel density of 0.68 per mm^3. This in vivo imaging technique was able to detect tubular structures down to 250 μm diameter with almost perfect accuracy (volume overlap ratio ~1) and down to 200 μm diameter with fair overlap (volume overlap ratio of 0.2) in a virtual phantom. Furthermore, this method was applied to study differences in intracortical vasculature in the tibia between subjects with type 2 diabetes and non-diabetic controls [43]. Diabetics showed significantly larger intracortical vessels with diameters of 272 ± 34.1 μm compared to controls with 258 ± 23.0 μm (p=0.046) [unpublished data].

Investigating associations with clinically diagnosed microvascular disease (retinopathy, nephropathy, or neuropathy), a significantly larger number of smaller vessels was observed in subjects with microvascular disease (Fig. 3) compared to those without (0.11 more vessels per mm^3, p=0.033, and 14.6 μm decreased average vessel diameter, p=0.048, in subjects with microvascular disease adjusting for age, sex, and body mass index, respectively). This association was paralleled by significantly higher cortical porosity and lower cortical bone mineral density (BMD) in subject with microvascular disease (cortical porosity: 9.98 ± 5.19% vs. 7.60 ± 2.43%, p=0.025; cortical BMD: 817 ± 93.5 cm^{-3} vs. 859 ± 57.2 cm^{-3}, p=0.033).

Bone perfusion in aging and disease

When individual vessels cannot be resolved, DCE-MR perfusion imaging can be used as a surrogate of vascularization. It provides information about tissue perfusion, vessel permeability, and extravascular-extracellular space [44]. Feasibility of in vivo perfusion imaging in cortical bone of rabbits and humans was demonstrated using DCE-MRI with UTE and IR-UTE sequences on a clinical 3T scanner [32]. MR data was acquired in single axial slices of 10 cm thickness in the tibial diaphysis of three healthy male volunteers. Using UTE-IR sequences a volume transfer constant K^{trans}= 0.23 min^{-1} and a time constant k_{ep}= 0.58 min^{-1} were reported in a 38-year-old volunteer. Comparing a 40-year-old and a 68-year-old man, the younger subject show approximately 2-fold higher maximum enhancement and 5- to 6-fold higher enhancement slope [32]. These case studies indicate how perfusion change in cortical bone could be monitored in vivo using MRI. Previous studies showed how bone perfusion declined with age [45] and in diseases, such as osteoporosis [46,47] and type 2 diabetes [48]. Decreased blood flow was linked to bone loss in older women [49] and to decreased material properties in aging rats [50].

Conclusion

We reviewed current MR-based techniques that allow in vivo assessment of intracortical vasculature, including ultra-short echo time UTE-MRI, DCE-MRI, and susceptibility-weighted MRI. Further, we presented preliminary studies that apply these techniques to investigate changes in intracortical vessels in aging and disease. The development of in vivo techniques for intracortical vessel visualization and characterization will enable the exploration of interactions between the vascular and skeletal systems, and further our understanding of drivers of cortical pore expansion. As we investigate potential pathways of cortical pore expansion, appropriate treatment and prevention strategies will be clarified.

Acknowledgements

None.

Financial support and sponsorship

This work was supported by the National Institutes of Health (NIH), National Institute of Arthritis and Musculoskeletal and Skin Diseases (NIAMS) with grants R01AR069670, R03AR064004, R01AR076159.

References

1. Ural A, Vashishth D. Effects of intracortical porosity on fracture toughness in aging human bone: a microCT-based cohesive finite element study. J Biomech Eng 2007; 129:625–631. [PubMed: 17887887]
2. Currey JD. The effect of porosity and mineral content on the Young's modulus of elasticity of compact bone. J Biomech 1988; 21:131–139. [PubMed: 3350827]
3. Schaffler MB, Burr DB. Stiffness of compact bone: effects of porosity and density. J Biomech 1988; 21:13–16. [PubMed: 3339022]
4. McCalden RW, McGeough JA, Barker MB et al. Age-related changes in the tensile properties of cortical bone. The relative importance of changes in porosity, mineralization, and microstructure. J Bone Joint Surg Am 1993; 75:1193–1205. [PubMed: 8354678]
5. Kawai M, de Paula FJA, Rosen CJ. New insights into osteoporosis: the bone-fat connection. J Intern Med 2012; 272:317–329. [PubMed: 22702419]
6. Brandi ML, Collin-Osdoby P. Vascular biology and the skeleton. J Bone Miner Res Off J Am Soc Bone Miner Res 2006; 21:183–192.
7. Garita B, Maligro J, Sadoughi S et al. Microstructural abnormalities are evident by histology but not HR-pQCT at the periosteal cortex of the human tibia under CVD and T2D conditions. Med Nov Technol Devices 2021; 10:100062. [PubMed: 37383338]
8. Leahy B, Garita B, Wu P-H et al. 2019 In vivo detection of vasculature and fat within cortical bone pores: a validation study. J Bone Miner Res 34 (Suppl 1). Available at https://www.asbmr.org/meetings/annualmeeting/AbstractDetail?aid=eeb2329f-59bd-41f2-a54d-a115399ad037. Accessed May 20, 2023.
9. Chen Q, Shou P, Zheng C et al. Fate decision of mesenchymal stem cells: adipocytes or osteoblasts? Cell Death Differ 2016; 23:1128–1139. [PubMed: 26868907]
10. Lewis JW, Edwards JR, Naylor AJ et al. Adiponectin signalling in bone homeostasis, with age and in disease. Bone Res 2021; 9:1. [PubMed: 33414405]
11. Tuckermann J, Adams RH. The endothelium-bone axis in development, homeostasis and bone and joint disease. Nat Rev Rheumatol 2021; 17:608–620. [PubMed: 34480164] ** Comprehensive review of endothelial cells in bone vasculature, signaling pathways that control angiogenesis, interaction between osteoclasts and endothelial cells, and how these mechanisms are affected by disease and aging.
12. Chen M, Li Y, Huang X et al. Skeleton-vasculature chain reaction: a novel insight into the mystery of homeostasis. Bone Res 2021; 9:21. [PubMed: 33753717]
13. Kusumbe AP, Ramasamy SK, Adams RH. Coupling of angiogenesis and osteogenesis by a specific vessel subtype in bone. Nature 2014; 507:323–328. [PubMed: 24646994]
14. Andreasen CM, El-Masri BM, MacDonald B et al. Local coordination between intracortical bone remodeling and vascular development in human juvenile bone. Bone 2023; 173:116787. [PubMed: 37150243] ** This study used a combination of histology and micro-ct with immunostaining to showed differences in vasculature in quiescent and non-quiescent pores and how vascular endothelial growth factor-A could play an import role in remodeling events.
15. Marenzana M, Arnett TR. The Key Role of the Blood Supply to Bone. Bone Res 2013; 1:203–215. [PubMed: 26273504]
16. Grüneboom A, Hawwari I, Weidner D et al. A network of trans-cortical capillaries as mainstay for blood circulation in long bones. Nat Metab 2019; 1:236–250. [PubMed: 31620676]
17. Herisson F, Frodermann V, Courties G et al. Direct vascular channels connect skull bone marrow and the brain surface enabling myeloid cell migration. Nat Neurosci 2018; 21:1209–1217. [PubMed: 30150661]
18. Kerschnitzki M, Wagermaier W, Roschger P et al. The organization of the osteocyte network mirrors the extracellular matrix orientation in bone. J Struct Biol 2011; 173:303–311. [PubMed: 21081167]
19. Standring S, Borley NR, Gray H, eds. Chapter 6 - Smooth muscle and the cardiovascular and lymphatic systems. In: Gray's anatomy: the anatomical basis of clinical practice. 40th edition . Edinburgh: Churchill Livingstone/Elsevier; 2008.

20. Betts JG, Desaix P, Johnson E et al. Anatomy & Physiology Available at https://openstax.org/details/books/anatomy-and-physiology. Houston, TX: OpenStax; 2017.
21. Hemmatian H, Laurent MR, Ghazanfari S et al. Accuracy and reproducibility of mouse cortical bone microporosity as quantified by desktop microcomputed tomography. PloS One 2017; 12:e0182996. [PubMed: 28797125]
22. Zeitoun D, Caliaperoumal G, Bensidhoum M et al. Microcomputed tomography of the femur of diabetic rats: alterations of trabecular and cortical bone microarchitecture and vasculature-a feasibility study. Eur Radiol Exp 2019; 3:17. [PubMed: 30972589]
23. Núñez JA, Goring A, Hesse E et al. Simultaneous visualisation of calcified bone microstructure and intracortical vasculature using synchrotron X-ray phase contrast-enhanced tomography. Sci Rep 2017; 7:13289. [PubMed: 29038597]
24. Salles S, Shepherd J, Vos HJ et al. Revealing Intraosseous Blood Flow in the Human Tibia With Ultrasound. JBMR Plus 2021; 5:e10543. [PubMed: 34761147]
25. Du J, Iori G, Raum K. Imaging of cortical pores using ultrasound contrast agents: Phantom and ex vivo studies. 2017 IEEE International Ultrasonics Symposium (IUS), 2017, 1–4.
26. Du J, Bydder GM. Qualitative and quantitative ultrashort-TE MRI of cortical bone. NMR Biomed 2013; 26:489–506. [PubMed: 23280581]
27. Jerban S, Ma Y, Moazamian D et al. MRI-based porosity index (PI) and suppression ratio (SR) in the tibial cortex show significant differences between normal, osteopenic, and osteoporotic female subjects. Front Endocrinol 2023; 14:1148345. ** This study applied porosity index (PI) and suppression ratio (SR) metrics to document significant differences among subjects of varying bone quality.
28. Jerban S, Chang DG, Ma Y et al. An Update in Qualitative Imaging of Bone Using Ultrashort Echo Time Magnetic Resonance. Front Endocrinol 2020; 11:555756.
29. Rajapakse CS, Bashoor-Zadeh M, Li C et al. Volumetric Cortical Bone Porosity Assessment with MR Imaging: Validation and Clinical Feasibility. Radiology 2015; 276:526–535. [PubMed: 26203710]
30. Li C, Seifert AC, Rad HS et al. Cortical bone water concentration: dependence of MR imaging measures on age and pore volume fraction. Radiology 2014; 272:796–806. [PubMed: 24814179]
31. Gordon Y, Partovi S, Müller-Eschner M et al. Dynamic contrast-enhanced magnetic resonance imaging: fundamentals and application to the evaluation of the peripheral perfusion. Cardiovasc Diagn Ther 2014; 4:147–164. [PubMed: 24834412]
32. Wan L, Wu M, Sheth V et al. Evaluation of cortical bone perfusion using dynamic contrast enhanced ultrashort echo time imaging: a feasibility study. Quant Imaging Med Surg 2019; 9:1383–1393. [PubMed: 31559167]
33. Wu P-H, Gibbons M, Foreman SC et al. Cortical bone vessel identification and quantification on contrast-enhanced MR images. Quant Imaging Med Surg 2019; 9:928–941. [PubMed: 31367547]
34. Liu C, Li W, Tong KA et al. Susceptibility-weighted imaging and quantitative susceptibility mapping in the brain. J Magn Reson Imaging JMRI 2015; 42:23–41. [PubMed: 25270052]
35. Dymerska B, Bohndorf K, Schennach P et al. In vivo phase imaging of human epiphyseal cartilage at 7 T. Magn Reson Med 2018; 79:2149–2155. [PubMed: 28758241]
36. Martel G, Kiss S, Gilbert G et al. Differences in the vascular tree of the femoral trochlear growth cartilage at osteochondrosis-susceptible sites in foals revealed by SWI 3T MRI. J Orthop Res Off Publ Orthop Res Soc 2016; 34:1539–1546.
37. Nissi MJ, Toth F, Zhang J et al. Susceptibility weighted imaging of cartilage canals in porcine epiphyseal growth cartilage ex vivo and in vivo. Magn Reson Med 2014; 71:2197–2205. [PubMed: 23857631]
38. Nissi MJ, Tóth F, Wang L et al. Improved Visualization of Cartilage Canals Using Quantitative Susceptibility Mapping. PloS One 2015; 10:e0132167. [PubMed: 26168296]
39. Wang L, Nissi MJ, Toth F et al. Quantitative susceptibility mapping detects abnormalities in cartilage canals in a goat model of preclinical osteochondritis dissecans. Magn Reson Med 2017; 77:1276–1283. [PubMed: 27018370]

40. Johnson CP, Wang L, Tóth F et al. Quantitative susceptibility mapping detects neovascularization of the epiphyseal cartilage after ischemic injury in a piglet model of legg-calvé-perthes disease. J Magn Reson Imaging JMRI 2019; 50:106–113. [PubMed: 30556613]

41. Ladd ME, Bachert P, Meyerspeer M et al. Pros and cons of ultra-high-field MRI/MRS for human application. Prog Nucl Magn Reson Spectrosc 2018; 109:1–50. [PubMed: 30527132]

42. Grüneboom A, Kling L, Christiansen S et al. Next-generation imaging of the skeletal system and its blood supply. Nat Rev Rheumatol 2019; 15:533–549. [PubMed: 31395974]

43. Loeffler MT, Wu P-H, Pirmoazen AM et al. 2022 Association between Dynamic Contrast-Enhanced MR-Derived Vessel Metrics and Microvascular Health in Patients with Type 2 Diabetes. J Bone Miner Res 38 (Suppl 1). Available at https://www.asbmr.org/meetings/annualmeeting/AbstractDetail?aid=c123bba1-aa93-48d5-8141-65a4ac2af2b8. Accessed May 20, 2023. * This is the first study on a small cohort of type 2 diabetics and healthy controls that used dynamic contrast-enhanced MRI to show differences in tibial bone vasculature in vivo.

44. Essig M, Shiroishi MS, Nguyen TB et al. Perfusion MRI: the five most frequently asked technical questions. AJR Am J Roentgenol 2013; 200:24–34. [PubMed: 23255738]

45. Prisby RD, Ramsey MW, Behnke BJ et al. Aging reduces skeletal blood flow, endothelium-dependent vasodilation, and NO bioavailability in rats. J Bone Miner Res Off J Am Soc Bone Miner Res 2007; 22:1280–1288.

46. Wang Y- XJ, Griffith JF, Kwok AWL et al. Reduced bone perfusion in proximal femur of subjects with decreased bone mineral density preferentially affects the femoral neck. Bone 2009; 45:711–715. [PubMed: 19555783]

47. Zhu J, Zhang L, Wu X et al. Reduction of Longitudinal Vertebral Blood Perfusion and Its Likely Causes: A Quantitative Dynamic Contrast-enhanced MR Imaging Study of a Rat Osteoporosis Model. Radiology 2017; 282:369–380. [PubMed: 27541685]

48. Stabley JN, Prisby RD, Behnke BJ et al. Type 2 diabetes alters bone and marrow blood flow and vascular control mechanisms in the ZDF rat. J Endocrinol 2015; 225:47–58. [PubMed: 25817711]

49. Vogt MT, Cauley JA, Kuller LH et al. Bone mineral density and blood flow to the lower extremities: the study of osteoporotic fractures. J Bone Miner Res Off J Am Soc Bone Miner Res 1997; 12:283–289.

50. Bloomfield SA, Hogan HA, Delp MD. Decreases in bone blood flow and bone material properties in aging Fischer-344 rats. Clin Orthop 2002;248–257.

Key Points:

1. In vivo techniques for intracortical vessel visualization and characterization support the exploration of interactions between the vascular and skeletal systems, and further our understanding of drivers of pathological cortical porosity.
2. The two main components of intracortical pore space are adipocytes and vessels; therefore, the assumption that intracortical porosity is equivalent to vascular space, and that probing water content (as in UTE MRI) provides an adequate measure of porosity, may be invalid.
3. Ultra-short echo time MRI (UTE MRI), dynamic contrast enhanced MRI (DCE-MRI), and susceptibility-weighted MRI techniques have been used to probe intracortical vasculature in vivo.
4. DCE-MRI was able to detect significant differences in vessel size and distribution secondary to type 2 diabetes and microvascular disease.

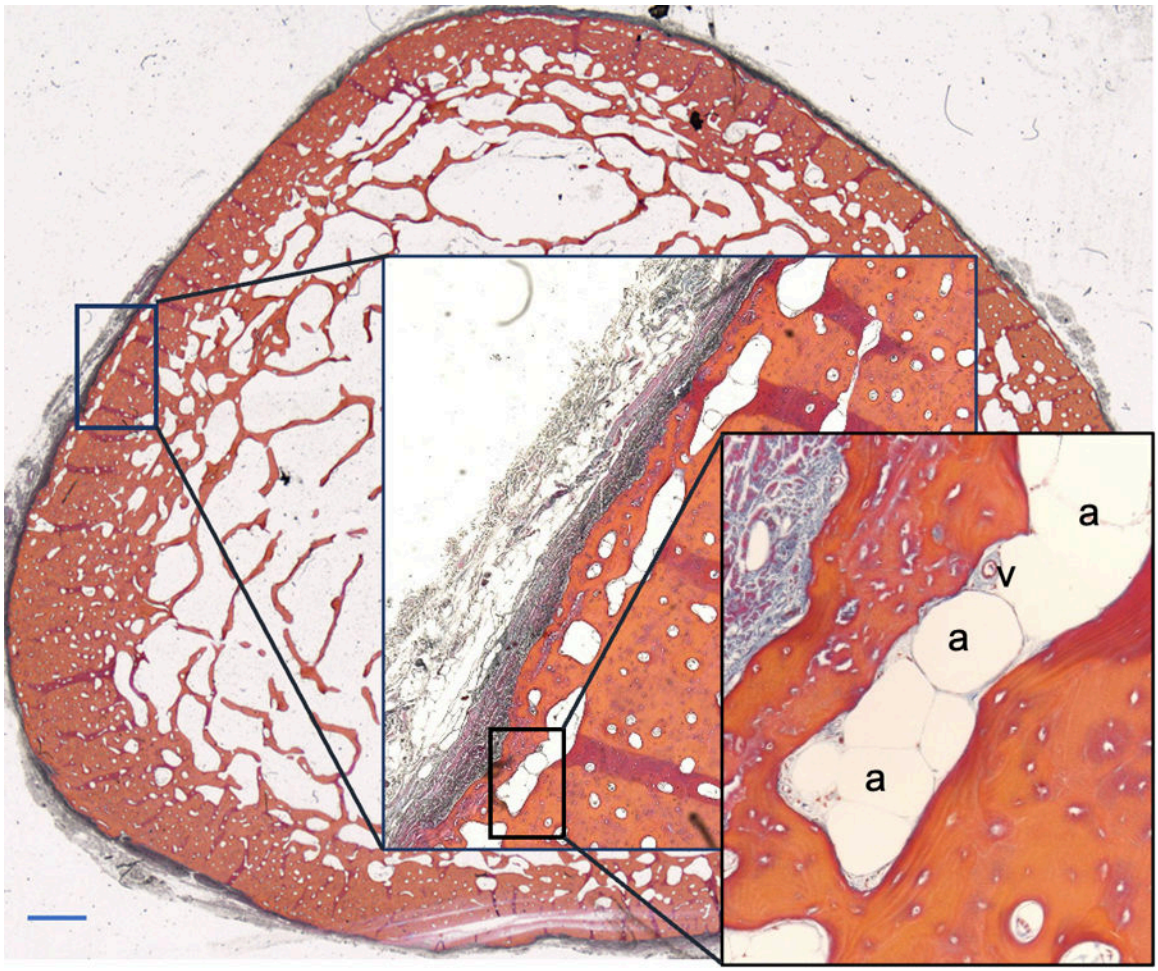

Fig. 1:

Tibia cross section from a 79-year-old donor with cardiovascular disease and type 2 diabetes (duration over 10 years). Intracortical pore space adipocytes labeled ‘a’, vessels labeled ‘v’. Scale bar= 2.5 mm. [original]

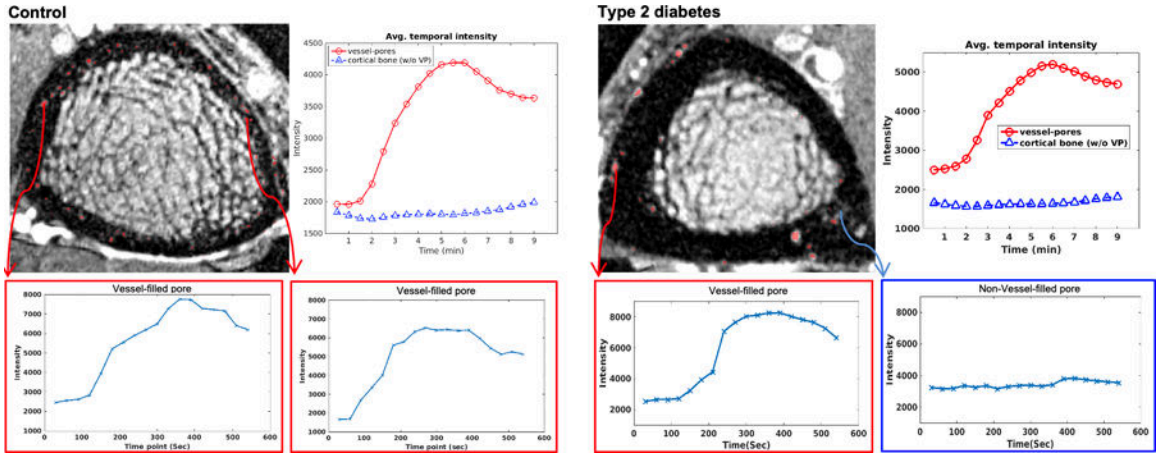

Fig. 2:

Representative results of the DCE-MRI vessel detection algorithm in a control participant (left) and participant with type 2 diabetes (right). Voxels identified as vessel-filled pores (red boxes) display signal enhancement, while non-vessel filled pores (blue boxes) do not. Enhancement curves are shown for individual pores (bottom row) and as average intensity for all detected vessel-filled and non-vessel-filled pores (above). [original]

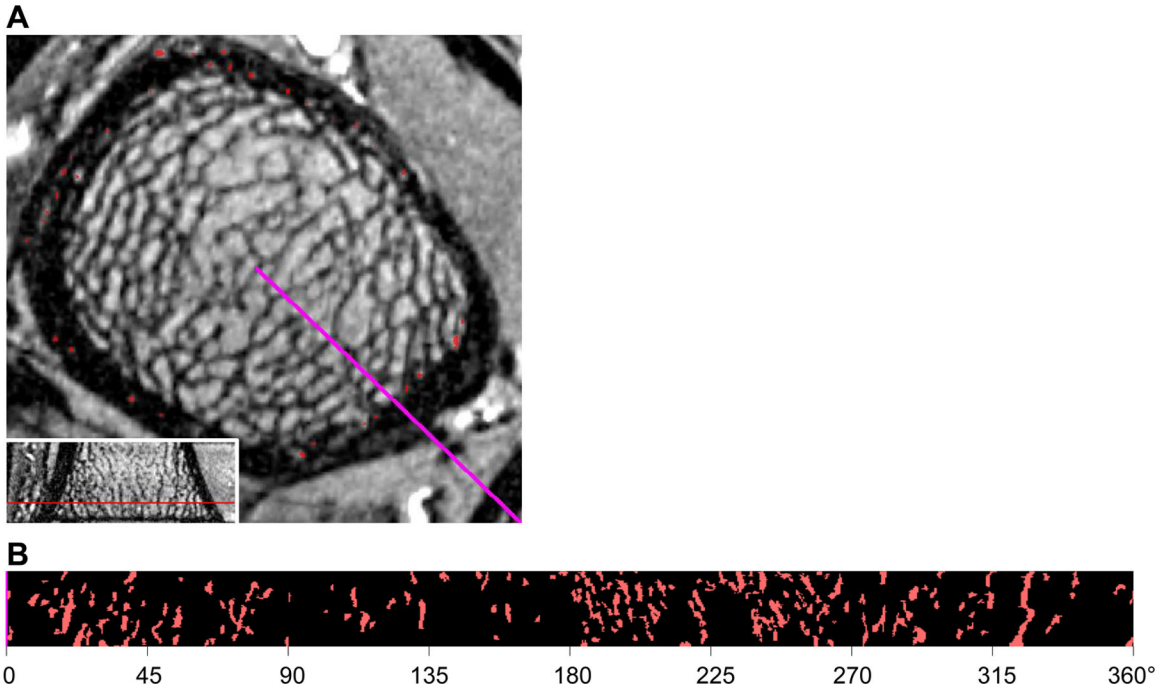

Fig. 3:

DCE-MRI of ultra-distal tibia of a 69-year-old woman with type 2 diabetes and neuropathy. Red voxels in axial view (A) represent detected intracortical vessels. Radial maximum intensity projection (MIP, B) shows a high density (0.18 per mm^3) of smaller intracortical vessels (246 μm average vessel diameter). Purple line in axial view marks 0° in MIP.

Table 1:

Types and sizes of human blood vessels

Type	Diameters [19,20]
Aorta and elastic arteries	10–30 mm
Muscular arteries (distributing arteries)	100 μm–10 mm
Arterioles	About 10 μm
Capillaries (single layer of ECs, no SMCs)	4–8 μm
Post-capillary venules (single layer of ECs, no SMCs)	10–30 μm
Muscular venules	About 50 μm or larger

Note. Except for capillaries and post-capillary venules that are distinct from other vessels by their histological composition there is a gradual transition between vessel types. EC= endothelial cells, SMC= smooth muscle cells